Detailed atomic structure of arbitrary fcc [100] twist grain boundaries

D. Romeu, L. Beltrán-del-Rio, J. L. Aragón, and A. Gómez
Instituto de Física, Universidad Nacional Autónoma de México, Apartado Postal 20-364, 01000 México, Distrito Federal, Mexico
(Received 24 June 1998; revised manuscript received 25 September 1998)

The generalized coincidence site network model has been applied to the study of fcc twist [100] grain boundaries. The result has been the detailed atomistic description of general (100) twist grain boundaries, supported by a set of quantitative expressions obtained directly from the model's hypotheses concerning primary and secondary dislocation spacings and Burgers vectors; these are in complete agreement with both accepted theory and experimental observations. According to the model, singular boundaries, defined as those boundaries containing only one primary dislocation per coincidence site lattice unit cell, are proposed to be composed of atomic domains with the structure of $\Sigma 1$, separated by an array of perfect primary dislocations. Every random boundary has an associated singular boundary and its structure consists of a mixture of domains found in the associated boundary, in different translational states; these domains are in turn separated by an array of partial secondary dislocations. A nonsingular boundary therefore contains arrays of both primary and secondary dislocations. [S0163-1829(99)07803-0]

I. INTRODUCTION

Most technological applications of metals involve their use in polycrystalline form. Since many properties of polycrystals depend strongly on phenomena occurring at grain boundaries (GB's), there has been a vast amount of work in the past decades attempting to relate the GB structure and properties. A major part of this work has been devoted to the development of geometrical criteria (not explicitly taking into account the physical interaction between atoms at the interface[1]) directed at obtaining information about the atomic structure of a GB given the macroscopic degrees of freedom that define the relative orientation of the parent crystals and the boundary plane. Although most available models, such as those based on the coincidence site lattice (CSL), the *O* lattice, and the displacement shift complete (DSC) lattice, have succeeded in accounting for the properties of singular GBs (GBs with special properties), they have failed to provide their detailed atomic structure, which has had to be inferred from computer simulations. Although such calculations have provided important insight into the relation between the GB structure and properties,[2] they are restricted by their discrete nature. Thus the general problem of relating the structure and properties of arbitrary (random) boundaries, by far the most abundant, has had limited attention, which has been one factor preventing the development of the field of grain boundary crystallography.

Recently, a structural model that could aid in the solution of the above limitation, called the generalized coincidence site network (GCSN), has been introduced.[3,4] The GCSN model generalizes the coincidence site lattice model[5] by replacing the strict coincidence criterion by one of quasicoincidence. This definition allows the study of grain boundaries using the mathematical framework developed in recent years for quasicrystals,[6] thus unifying both fields. The quasicoincidence criterion on its own, however, is not what makes the GCSN distinct and useful; the model's key feature lies in the way in which grain boundaries (bicrystals) are built. Contrary to the usual construction of merely juxtaposing two crystal slabs, GCSN bicrystals have a distinct GB volume with atoms at positions determined by quasicoincident sites, which are assumed to minimize the elastic energy at the interface, a hypothesis to be verified *a posteriori* both empirically and numerically.

Although the GCSN model contains an explicit assumption concerning atomic relaxations at the interface, so that it cannot be considered as purely geometrical,[1] it cannot predict which GBs will turn out to have comparatively lower energies. The model merely supplies a starting atomic configuration for each GB that is expected to be near a local minimum for most common (central) potentials used to model fcc metals. To determine which boundaries are energetically preferred, one must perform atomistic calculations on GCSN bicrystals using a suitable potential. Such calculations, performed using a variety of potentials,[7–10] have shown[11] that indeed GCSN bicrystals are, for all the potentials used, close to an energy minimum and that the original structure remains basically unaltered upon relaxation. However, although the relaxed structures obtained from different potentials are basically indistinguishable from one another, the actual energy vs misorientation curves show substantial differences, even for the same metal.[11] For this reason, although GCSN structures are found to be stable for all the potentials tried, the final assessment must be based on their ability to account for actual experimental observations rather than computer simulations.

This paper contains a set of results obtained from the application of the GCSN model to the study of fcc twist [100] grain boundaries under the hypothesis that there are at least some real systems ''affine'' to the model whose interatomic potentials minimize interfacial energy as proposed by the model and whose structure is therefore well represented by it. The fact that the structure of GCSN bicrystals remains basically unaltered upon relaxation, preliminarily supports this hypothesis, although the strongest piece of evidence is provided by the quantitative results described in this paper.

In the following sections it will be shown that GCSN grain boundaries reproduce quantitatively important experimental observations about the structure of primary and secondary GB dislocation networks. We also introduce a defi-

nition of singularity based on minimum dislocation content and report other fundamental predictions concerning the detailed atomic structure of singular (delimiting) and random (intervening) boundaries, as well as the angular range over which the structure of delimiting boundaries extends.

II. GCSN MODEL

In what follows we shall give a brief nonmathematical description of the GCSN model for self-containment purposes. For a more rigorous treatment the reader is referred to previously published papers.[6,4]

A. GCSN bicrystal

The coincidence site lattice model,[5] considers points common to both lattices as points of good fit and assumes that special boundaries arise when the reciprocal of the density of coincidence sites (denoted by Σ) is low. The GCSN model is also defined as a set of points of good fit between two lattices, but here the strict coincidence requirement of the CSL is replaced by one of ''quasicoincidence'' defined as follows. Two points (one in each lattice) are quasicoincident if they both lie in the intersection of their respective Wigner-Seitz cells. A more intuitive definition is that two points, or sites, are quasicoincident if each is the only nearest neighbor of the other and their distance is less than the sum of the radii of the atoms that occupy the sites. The GCSN is then defined as the set of middle or average points between quasicoincident pairs. It must be noted that although the term lattice has been used, the definition of the GCSN does not require the interpenetrating structures to be periodic, thus allowing the construction of crystal-quasicrystal and quasicrystal-quasicrystal interfaces.

Since the quasicoincidence criterion is obviously met by strictly coincident points, the GCSN contains the associated CSL, but more importantly it also contains its decoration (see Fig. 4). Thus, for decorated lattices the GCSN yields the detailed atomic structure of the boundary including the primary and secondary dislocation networks. Note that in contrast to the CSL, the GCSN remains well defined when the tangent of the misorientation angle is irrational, although in this case the GCSN set will be an aperiodic network rather than a lattice.[3,6]

A GCSN bicrystal is built as follows. (a) Two arbitrary lattices are brought together with a common origin and one of them is rotated through a given axis/angle pair. Optionally, one of the lattices can be further displaced by an arbitrary vector. (b) A boundary slab with nonzero thickness (the GB thickness is normally set to one interplanar spacing) is defined passing through the origin for convenience. (c) All lattice points inside the boundary are replaced by the GCSN set as defined above. (d) All remaining points of lattice 1 (lattice 2) above (below) the boundary are removed, leaving only the points of lattice 2 (lattice 1) that have not been used to generate a GCSN point in the boundary.

In the specific case of twist boundaries with low index rotational axes, all boundary atoms lie on a single plane [Figs. 1(b) and 3]. On the other hand, when the boundary normal is not a low index crystallographic plane, the prerelaxed boundary zone may have finite thickness, as shown in Fig. 1(c).

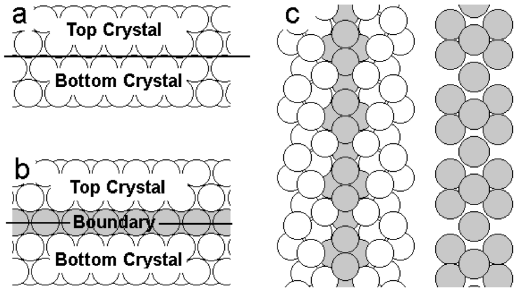

FIG. 1. (a) Common bicrystal construction with two juxtaposed crystal slabs. (b) GCSN bicrystal with a distinct boundary region (in gray). (c) Left, tilt bicrystal with boundary atoms in gray; right, side view of boundary atoms.

B. Elastic energy minimization

It must be noted that the above prescription differs from the one commonly used to model bicrystals,[12] where two crystal slabs are just juxtaposed on either side of the boundary as shown in Fig. 1(a). Thus, in contrast to the usual construction, the prerelaxed boundary in a GCSN bicrystal contains atomic sites that, except for coincidences, do not belong to either crystal.[13]

This difference is crucial and lies at the heart of the model. In a GCSN bicrystal, every atom in the boundary is located at the middle point between two quasicoincident sites (overlapping atoms) from the parent lattices. The middle point is a compromise location between the slightly different positions each crystal atom would occupy in its own lattice if there were no interface. This causes the atoms in the boundary to act as an elastic cushion that provides a smooth transition between the two adjacent crystals. As a result, when a GCSN bicrystal is relaxed, the atoms in the boundary and nearby crystals change their positions only very slightly (see Fig. 2), leaving the GB structure practically unaltered.[11]

Based on the above, the GCSN model should provide a fair representation of the GB structure of any system for which the GCSN energy minimizing mechanism holds true (presumably most close packed metals) or any system whose structure can be modeled by a central potential. Although,

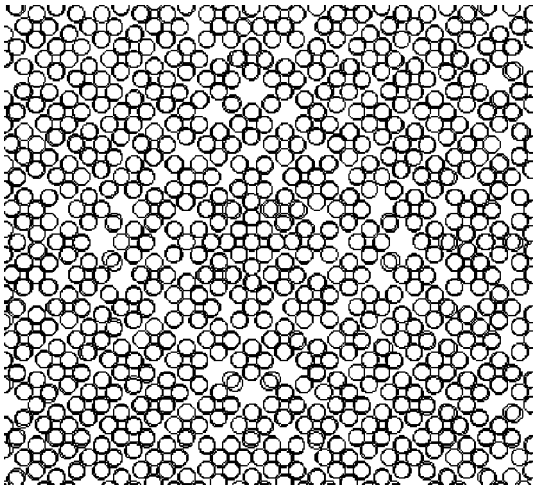

FIG. 2. Superimposed plots of atoms in the random boundary ($\theta = 23.62°$) before and after static relaxation carried out using the Ni potential of Bristowe and Crocker.

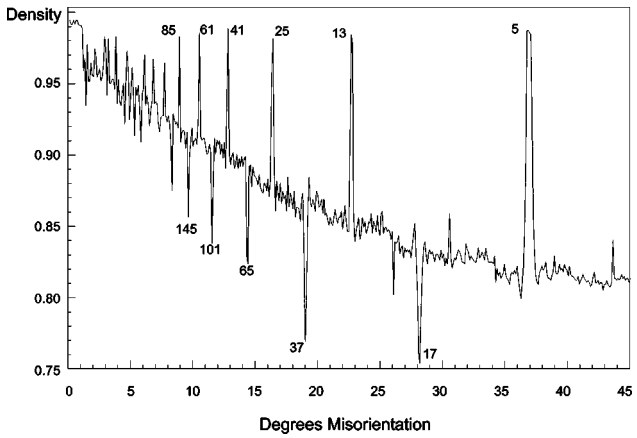

FIG. 3. Normalized plot of the atomic density vs the misorientation angle in degrees for fcc [100] twist boundaries calculated every one-hundredth of a degree. The numbers next to the peaks identify the corresponding values of Σ.

we reiterate, a final assessment of the validity of this statement and the determination of what systems are well described by the model requires the comparison of the predictions of the model with experimental observations. For all such systems, the GCSN model allows the basic structural features of their GBs to be studied without recourse to computer calculations, making it possible to perform crystallographic studies on arbitrarily large boundaries over the whole angular range.

III. STRUCTURE OF SINGULAR BOUNDARIES

A. Primary dislocations

As an example of a useful calculation that can now be performed over the whole angular range, Fig. 3 shows a plot of the GB atomic density vs misorientation angle for fcc [100] twist boundaries, calculated with an accuracy of one-hundredth of a degree. The plot describes the number of GB sites (quasicoincident pairs) found in a fixed circular section of the boundary plane with a diameter of 30 lattice spacings.

Note that the plot, which properly normalized describes all cubic lattices, has sharp peaks and troughs at specific coincidence misorientations with the values of Σ indicated in the figure. Although at this point, no physical significance is attributed to this plot other than being a measure of the good fit or registry between two rotated (100) crystal planes, it turns out that both major peaks and troughs reproduce the orientations of low-energy singular boundaries found in some real systems. This is evidenced by the fact that they coincide with the orientations identified as most probable in MgO twist bicrystal experiments.[14,15] Although these experimental results differ somewhat, the highest observed frequencies coincide with the peaks and troughs of Fig. 3. Assuming that these orientations identify special (singular) boundaries, if a physical property could be found that distinguishes them from all others, it could be possible to establish a definition of singularity that might prove to be valid for all cubic (100) twist boundaries.

According to Ranganathan,[16] a CSL is generated when one lattice is rotated with respect to the other around an axis $\langle h,k,l\rangle$ through the angle

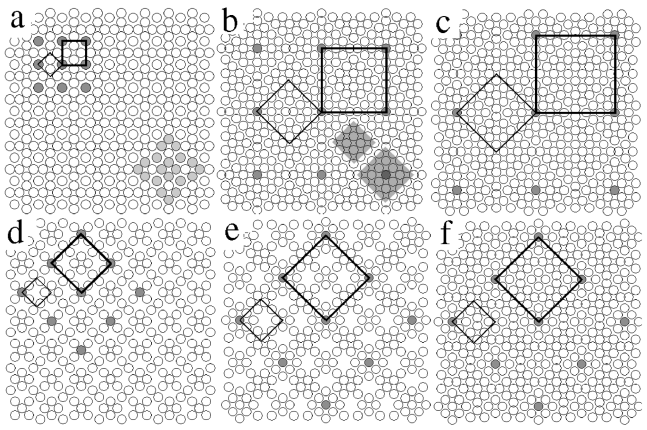

FIG. 4. (a)–(e) Atomic structures of $\Sigma 5, \Sigma 41, \Sigma 61, \Sigma 17$, and $\Sigma 37$, respectively. (f) $\Sigma 37$ with vacant sites removed. Open circles: normal GB atoms; dark gray circles, CSL nodes; thin lines, *O* lattice unit cell; thick lines, CSL unit cell. Light gray atoms in $\Sigma 5$ mark atomic patterns also found in $\Sigma 17$. Dark squares in $\Sigma 41$ ($n=4$) highlight atomic domains with four and five atoms on the edge.

$$\theta = 2\tan^{-1}\left(\sqrt{N}\frac{y}{x}\right), \tag{1}$$

with x and y relatively prime integers, $N=h^2+k^2+l^2$, and $\Sigma = x^2+Ny^2$ (divided by two until Σ is odd). Using these definitions, major peaks in Fig. 3 ($N=1$) are found at angles θ_n for which $y=1$ and $x=2n+1$, while troughs occur when $x=2n$, $n=1,2,\ldots$. Therefore, all special orientations correspond to coincidence boundaries for which $y=1$ and $\Sigma_n = 2n^2+2n+1$ for peaks and $\Sigma_n = 4n^2+1$ for troughs. Equivalent results have been obtained for [110] and [111] twist and tilt boundaries, but they shall be described elsewhere.

It turns out that the calculated boundaries of all major peaks (x odd) are composed of square atomic domains disposed in a checkered pattern, containing n and $n+1$ atoms on the edge (see Fig. 4). As the misorientation angle increases, the size of the domains decreases from infinite at $\Sigma 1(\theta=0°)$ to the smallest possible square domains of $\Sigma 5(\theta=36.87°)$ with only one and two atoms on edge. This is exemplified in Figs. 4(a)–4(c) showing the structures of $\Sigma 5$, $\Sigma 41$, and $\Sigma 61$ ($n=1$, 4, and 5), respectively. In Fig. 4 the circles represent general GCSN atoms, with dark gray circles marking coincidence positions. The CSL and *O* lattice unit cells are also drawn with thick and thin lines, respectively. In the case of troughs [Figs. 4(d) and 4(e)], the boundary is also composed of a small number of atomic domains, but not all of them are square and some have vacant sites, which accounts for their low density. We shall discuss these vacancies below, but first we must make the important remark that all boundaries in Fig. 4 belong to the translational state defined as type 2 by Bristowe and Crocker.[17] The GCSN model always produces structures in this state when there is no relative translation between the parent lattices.

In terms of the integers x and y, the *O* lattice basis vectors are given (in the standard fcc basis with the Z coordinate omitted) by

$$\mathbf{O}_1=\frac{1}{4y}(x+y,y-x),$$
$$\mathbf{O}_2=\frac{1}{4y}(x-y,x+y). \tag{2}$$

When x and y have different parity (troughs), the CSL is parallel to the O lattice with basis vectors given by

$$\mathbf{c}_1=\frac{1}{2}(x+y,y-x),$$
$$\mathbf{c}_2=\frac{1}{2}(x-y,x+y). \tag{3}$$

When x and y are both odd (peaks), the CSL is inclined 45° to the O lattice and its unit cell vectors are

$$\mathbf{c}_1=\frac{1}{2}(x,y), \tag{4}$$
$$\mathbf{c}_2=\frac{1}{2}(y,-x).$$

Figure 4 shows that atomic domains always have an O point at their center and that they are delimited by an array line defects known as primary grain boundary dislocations. Here the GCSN model has passed its first test in reproducing the well known fact that primary dislocation lines lie along the edges of the Wigner-Seitz lattice of the O lattice and mark the regions where the atomic fit is at its worse.[18] A good measure of this misfit is the distance between the overlapping (quasicoincident) crystal atoms that gave rise to each GCSN atom in the boundary. This separation increases linearly from zero at the domain center to a maximum of half an atomic diameter at the domain edge, where the dislocation line lies. Note that, in accordance with Bollmann, the distance between primary dislocations in singular GCSN boundaries, and hence between domains, is a vector of the O lattice. Another point of agreement with established theory is that primary dislocations have crystalline Burgers vectors $\frac{1}{2}$ [110], as verified by performing a Burgers circuit going through both crystals.

B. Definition of singularity

Since the size ratios of the CSL and O lattice unit vectors are $2y$ and $\sqrt{2}y$ for the parallel and inclined states, respectively [Eqs. (2)–(4)], it follows that as y increases, so does the density of O points within the CSL unit cell, with the consequent decrease in domain size (good fit regions) and increase in primary dislocation content. It is then reasonable to assume that the boundaries for which $y=1$ owe their singularity to the fact that they have the smallest possible value of y and therefore the minimum dislocation content per CSL unit cell. Also, in Sec. IV we shall see that when $y>1$ (a general GB), an additional network of secondary dislocations appears in the boundary, increasing its complexity and presumably its energy.

Two important points must be kept in mind. Notwithstanding its variable size, all the domains found in special boundaries have the structure of a [100] crystal plane ($\Sigma 1$) and all special boundaries contain atomic patterns or two-dimensional structural units (2DSU's), found in adjacent special boundaries. To see this, compare the light gray atoms of $\Sigma 5$ in Fig. 4(a) with the atomic patterns of the adjacent special boundary $\Sigma 17$ in Fig. 4(d).

We shall now discuss the origin of the large differences in GB density. In the trivial situation ($\theta=0$), every atom in one crystal lattice is paired with exactly one fully coincident atom in the other. This means that when overlapping atoms are replaced by single atoms at intermediate points, the number of GCSN sites equals the number of atoms each crystal had in the intersection volume, i.e., in the GB region. In this case, the density of the GB is equal to that of the crystal, the maximum possible. In the general case, there is a number of atomic sites, which varies with the angle, that do not have a quasicoincident partner in the other lattice and cannot give rise to a GCSN atom. These ''orphan'' atoms are invariably located at positions where the atomic fit is worse and result in a void or vacancy near them. The peaks of Fig. 3 occur at the relative orientations for which the number of quasicoincident pairs is maximized, while at troughs, the contrary occurs.

It is possible to fill the voids in the boundary by repeating the quasicoincidence pairing process using only the sites that remained unpaired during the first iteration or by leaving the orphan atoms as part of the boundary. The result of carrying out such an operation is shown in Fig. 4(f), which is to be compared with its ''unfilled'' counterpart of Fig. 4(e). Although these extra atoms are too close to other boundary atoms, giving rise to zones of relatively high strain, calculations have shown[11] that a smaller energy value is often obtained when these sites are filled. However, due to the local strain at these sites, it is possible that even lower-energy values could be obtained if they are occupied by atoms of a different species; this would turn them into preferential sites for impurity segregation. If this is so, then low-density special boundaries might have different properties, such as diffusion coefficients, from the ones giving rise to peaks. This would imply that GB's that have a singular behavior under a given property such as minimum dislocation content may appear to be random under another. We are at present carrying out calculations to clarify this point.

IV. STRUCTURE OF RANDOM (GENERAL) BOUNDARIES

In what follows we will show that any random (nonsingular) GB can be associated with a singular boundary of the type described in the preceding section. We will then see that the structure of the arbitrary GB is composed of a mixture of the structural units of the associated singular boundary in different translational states.

A. Associated singular boundary

As it will become clear below, a useful insight into the structure of general GCSN boundaries can be obtained if one regards random boundaries as coincidence boundaries of arbitrarily long periods. Since the set of rational numbers is dense, any random GB with a measured misorientation angle θ_{arb} can be approximated, according to Eq. (1), to any degree of accuracy by $2\tan^{-1}(p/q)$ for some relatively prime

integers p and q; note that $N=1$ for the (100) twist case under consideration. This means that, given a tolerance, every GB can be thought of as a coincidence boundary with

$$\Sigma_{arb}=p^2+q^2 \tag{5}$$

if p and q have different parities and

$$\Sigma_{arb}=\frac{1}{2}(p^2+q^2) \tag{6}$$

otherwise. The decisive step is to express the ratio $r=p/q$ in terms of the integers x and c as

$$r\equiv r_{x,c,p}\equiv\frac{1}{x+c/p}, \tag{7}$$

with x defined as

$$x=\mathcal{R}\left[\frac{q}{p}\right]=\mathcal{R}\left[1\Big/\tan\left(\frac{\theta_{arb}}{2}\right)\right], \tag{8}$$

$\mathcal{R}[\ ]$ being the nearest integer function and c

$$c=q-px. \tag{9}$$

The positive integer x labels the singular ($y=1$) boundary Σ_x at the special misorientation angle

$$\theta_x=2\tan^{-1}\left(\frac{1}{x}\right) \tag{10}$$

that is to be associated to the arbitrary boundary $\Sigma_{arb}\equiv\Sigma_{x,c,p}$. If one writes the denominator of Eq. (7) as $x'=x+c/p$, then the term c/p (which need not be rational) represents a deviation parameter from the associated singular boundary Σ_x.

Given that the choice p,q is not unique, this approach would appear to lead to an ambiguous description of GB's. Experimentally, however, this is not the case since all relevant quantities will ultimately depend on the deviation parameter c/p and x, which are well defined quantities. The important point is that, theoretically, one has direct access to the internal variables p and c, which are directly related to the detailed structure of all twist GB's.

B. Structure of random boundaries

Assume that $\tan(\theta_{arb})$ is restricted to be a rational number and consider the sequence of coincidence boundaries $\{r_{x,c,p}\}$ obtained by varying p while keeping c and x fixed. At the one end, when $p=1$, $r_{x,c,1}=1/(x+c)$ and $\theta_{arb}=\theta_{x+c}$, which is by definition a singular boundary (Σ_{x+c}) since $x+c$ is an integer. At the other end, as $p\to\infty$, $r_{x,c,p}\to 1/x$ and $\theta_{arb}\to\theta_x$, which is the special boundary Σ_x associated with the random Σ_{arb}. Therefore, $\{r_{x,c,p}\}$ generates a sequence of (intervening) boundaries $\{\Sigma_{x,c,p}\}$ in the interval (θ_x,θ_{x+c}) between the special (delimiting) boundaries Σ_{x+c} and Σ_x. There is one such sequence for every value of c, although they have only formal interest since c (and hence the delimiting angle θ_{x+c}) cannot be determined experimentally and, as it will be seen shortly, the structure of any boundary is completely determined by the structure of the associated boundary Σ_x.

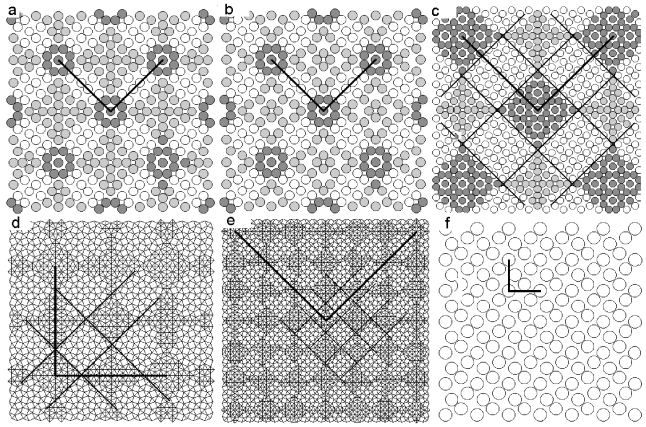

FIG. 5. Some GB's associated with $\Sigma 5$: (a) $\Sigma 53$ without vacancies, (b) $\Sigma 53$ with vacancies, (c) $\Sigma 185$, (d) and (e) wire frames of $\Sigma 461$ and $\Sigma 1189$ with lines joining atoms separated one lattice spacing or less, and (f) $\Sigma 5$ in the translational state type CSL. Gray atoms, atomic domains in the type 2 translational state; thick lines, CSL vectors; thin lines, average position of partial secondary GB dislocations.

Note that $\Sigma_{arb}\equiv\Sigma_{x,c,p}\to\infty$ as $\theta_{x,c,p}\to\theta_x$, which means that the period of intervening boundaries grows without limit as they approach θ_x. This should come as no surprise since, as we have seen, also the period of singular boundaries Σ_x diverges as $\theta_x\to 0$. This is a trivial result for singular boundaries and it means that the distance between primary dislocations, which is an increasing function Σ_x, grows without limit as one approaches $\Sigma 1$ at $\theta_x=0$. In the case of random boundaries, the distance between secondary dislocations is also an increasing function of the period $\Sigma_{x,c,p}$ and consequently it must also diverge upon approaching Σ_x.

From the comparative observation of GCSN twist boundaries over the whole angular range ($0°-45°$), a fundamental result emerges. Every nonsingular ($y>1$) GB is composed of a mixture of two sets of isostructural atomic domains arranged in a checkered pattern that has the periodicity of the nonsingular CSL ($\Sigma_{x,c,p}$). The domains in each set have the same structure of the associated Σ_x special boundary, but they are in different translational states.[17]

As an example, Fig. 5(a) shows the atomic structure of the nonsingular boundary $\Sigma 53\equiv\Sigma_{3,1,2}$ located at $\theta_{3,1,2}=31.89°$ between the singular boundaries $\Sigma 17\equiv\Sigma_4$ and $\Sigma 5\equiv\Sigma_3$. This boundary is the second ($p=2$) element of the sequence $\{\Sigma_{3,1,p}\}$ and is composed of two sets of atomic domains. For easy identification, the atoms in the first set have been filled with two levels of gray, while the atoms in the second set are represented with unfilled circles. Note that the domains of the first set have the structure of the $\Sigma 5$ type 2 boundary shown in Fig. 5(a), while those of the second set have the structure of $\Sigma 5$ type CSL, shown in detail in Fig. 5(f). This boundary was constructed using the same misorientation angle of $\Sigma 5$ ($36.87°$) but with one crystal shifted by the vector $\frac{1}{2}(\mathbf{d}_1+\mathbf{d}_2)$, where $\mathbf{d}_1=(3,1)/10$ and $\mathbf{d}_2=(1,-3)/10$ are the unit vectors of the associated $\Sigma 5$ DSC lattice.[19,17]

The DSC lattice basis vectors are the same vectors of the CSL [Eqs. (3) and (4)] divided by Σ and for singular boundaries they can be expressed as

$$\mathbf{d}_1=\frac{1}{x^2+1}(x,1),$$
$$\mathbf{d}_2=\frac{1}{x^2+1}(1,-x), \tag{11}$$

when x,y are both odd and

$$\mathbf{d}_1=\frac{1}{2(x^2+1)}(x+1,1-x)$$
$$\mathbf{d}_2=\frac{1}{2(x^2+1)}(x-1,x+1), \tag{12}$$

otherwise. In either case

$$|\mathbf{d}_1|=|\mathbf{d}_2|=(2\Sigma)^{-1/2}. \tag{13}$$

Figure 5(a) shows the random $\Sigma 53$ with its vacant sites filled. If the vacancies are not filled, the boundary structure looks as shown in Fig. 5(b), where one can see that the now incomplete light gray domains have the structure of $\Sigma 17 \equiv \Sigma_4$ of Fig. 4(d), which is also shown in its unfilled state. This is a general result. Every twist GB (with or without vacancies) contains a mixture of atomic patterns (2DSU's) from the two special boundaries θ_x and θ_{x+1} between which it lies, this being a direct consequence of the fact that every singular boundary Σ_x contains atomic patterns of $\Sigma_{x+1,}$ as described in Sec. III A.

The same conclusion is arrived at in the structural model of Vitek and Sutton[20] according to which all GB's in a certain misorientation range delimited by two short period GB's, are composed of mixtures of structural elements that belong to these boundaries. The delimiting boundaries are then called favored if they are not themselves, composed of units from other boundaries. In Vitek and Sutton's model, delimiting boundaries are assumed to be periodic boundaries with low Σ and their role is equivalent to the singular Σ_x boundaries of this work, although in our case, no restriction is made on the size of Σ_x, which can be very large for small-angle boundaries. This model was later extended to twist boundaries[21] and generalized for cubic systems.[22] Although the main assertion of the two models is identical, there are important differences, one of them being that delimiting boundaries are automatically produced by the GCSN model and do not have to be determined from considerations outside the model. Another important difference lies in the nature of the structural units, which is necessarily different due to the different models of bicrystal used. In particular, it would be very difficult to detect atomic domains in different translational states using the usual bicrystal construction.

C. Secondary grain boundary dislocations

The arrangement of the domains within the CSL depends only on x and c, i.e., on the particular sequence the random GB belongs to. All boundaries in a given sequence $\{\Sigma_{x,c,p}\}$ remain topologically identical as p increases, the only change being the size of the domains. This is exemplified in Fig. 5(c), which shows the fourth member ($p=4$) of the same ($x=3,c=1$) sequence: $\Sigma 185=\Sigma_{3,1,4}$ at $\theta_{3,1,4}=34.21°$. Note that the domains have increased in size, but their structure and relative position within the CSL have remained unchanged. Note also that adjacent domains always merge coherently, so that domain limits are not easily determined from a two-dimensional (2D) diagram alone.

To illustrate what the differences between different sequences, (different c) are, Figs. 5(d) and 5(e) show the boundaries $\Sigma 461\equiv\Sigma_{3,2,9}$, $\theta_{3,2,9}=34.48°$ and $\Sigma 1189 \equiv\Sigma_{3,3,9}$, $\theta_{3,3,9}=33.72°$, also associated with $\Sigma 5$ ($x=3$ for all of them) but belonging to the $c=2$ and $c=3$ sequences, respectively. In view of the large size of the CSL unit cell, these boundaries are shown as wire frames for clarity. Together, Figs. 5(a)–5(e) illustrate that there are always $|c|$ atomic domains of a given translational state along both the edge and diagonal of the CSL unit cell.

Since CSL type atomic domains appear after displacing one crystal lattice by $\mathbf{b}=\pm(\mathbf{d}_1\pm\mathbf{d}_2)/2$, the thin lines drawn between domains in Figs. 5(a)–5(e) represent dislocation lines with the Burgers vector $\mathbf{b}$. It is important to note that $\mathbf{d}_1$ and $\mathbf{d}_2$ belong to the DSC lattice of the singular boundary Σ_x, not to the DSC lattice of the arbitrary $\Sigma_{x,c,p}$, and that $\mathbf{b}$ is always parallel to the dislocation lines, which implies that these dislocations have a screw character, a fact that is in accordance with experimental observations.[19]

Using Eqs. (11) and (12), it can be seen that the Burgers vector $\mathbf{b}$ has a very simple expression (in the standard fcc lattice) in terms of the misorientation angle of the associated singular boundary θ_x:

$$\mathbf{b}_1=\frac{\mathbf{d}_1+\mathbf{d}_2}{2}=\frac{1}{2(x^2+1)}(x+1,1-x),$$
$$\mathbf{b}_2=\frac{\mathbf{d}_1-\mathbf{d}_2}{2}=\frac{1}{2(x^2+1)}(x-1,x+1), \tag{14}$$
$$|\mathbf{b}|=|\mathbf{b}_1|=|\mathbf{b}_2|=\frac{1}{\sqrt{2}}\sin\left(\frac{\theta_x}{2}\right)=\frac{1}{2\sqrt{\Sigma_x}}$$

for x odd and

$$\mathbf{b}_1=\frac{\mathbf{d}_1+\mathbf{d}_2}{2}=\frac{1}{x^2+1}(x,1),$$
$$\mathbf{b}_2=\frac{\mathbf{d}_1-\mathbf{d}_2}{2}=\frac{1}{x^2+1}(1,-x), \tag{15}$$
$$|\mathbf{b}|=|\mathbf{b}_1|=|\mathbf{b}_2|=\sin\left(\frac{\theta_x}{2}\right)=\frac{1}{\sqrt{\Sigma_x}}$$

otherwise. It is well known[18] that secondary dislocations with DSC Burgers vectors appear in arbitrary GB's as a result of the angular difference with a nearby special GB. Since $\mathbf{b}$ is not a DSC lattice vector, the dislocations in Fig. 5 cannot be perfect secondary dislocations but partials, and it is the stacking fault associated with partial dislocations that is responsible for the different structures of adjacent domains. Neighboring isostructural domains are themselves shifted with respect to each other by the vectors of the DSC

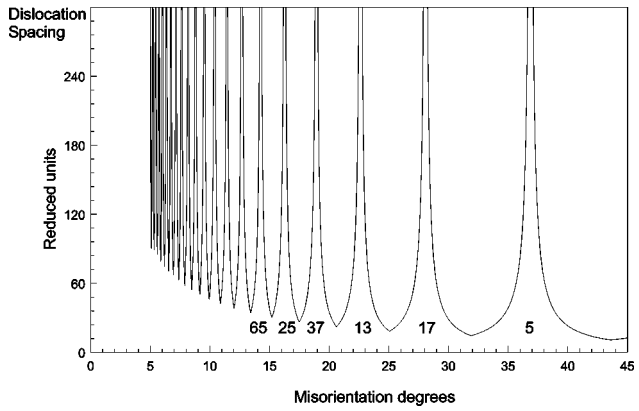

FIG. 6. Distance between secondary grain boundary dislocations in reduced units vs the misorientation angle. Note that the distance between dislocations diverges at the orientations of singular delimiting boundaries.

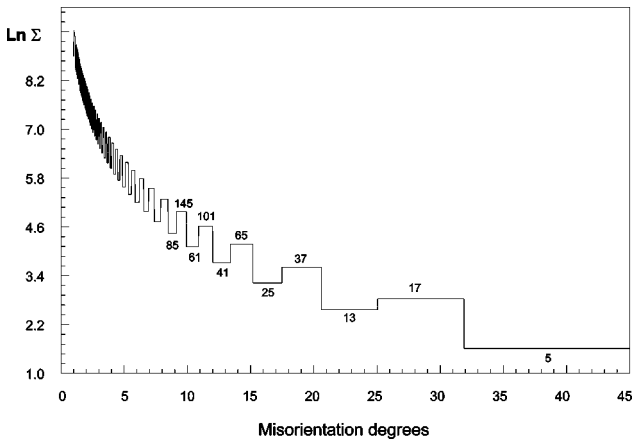

FIG. 7. Semilogarithmic plot of Σ_x versus the angle in degrees indicating the range over which the structure of singular boundaries is maintained in the two-dimensional structural units of fcc [100] twist grain boundaries.

lattice $\mathbf{d}_1$ and $\mathbf{d}_2$; hence the observed partial dislocations must be interpreted as the dissociation products of perfect secondary dislocations separating isostructural domains.

D. Secondary dislocations spacing

While discussing the structure of singular boundaries we mentioned that the relative sizes of the CSL and *O* lattice are given by $2p$ when the two lattices are inclined and $\sqrt{2}p$ when they are parallel. This means that there are exactly $2pO$ lattice vectors along the edge or diagonal of the CSL unit cell, depending on orientation, and that there are $|c|$ isostructural domains along both the edge and diagonal of the CSL cell. It then follows that the average distance between partial secondary dislocations (separating domains) is given by the reciprocal of the deviation parameter $|p/c|$ times the size of the *O* lattice basis vectors, i.e.,

$$\delta = |o|\left|\frac{p}{c}\right| = |o|\,\frac{\tan(\theta_{x,c,p}/2)}{1 - x\tan(\theta_{x,c,p}/2)}, \tag{16}$$

where $|o|$ is the size of the *O* lattice vectors and $\theta_{x,c,p}$ is the measured misorientation angle. With the aid of Eq. (2), Eq. (16) can be expressed in terms of the misorientation angle $\theta_{x,c,p}$ and the lattice parameter a as

$$\delta = \frac{\sqrt{2}a}{4}\left(\frac{1}{\cos(\theta_{x,c,p}/2) - x\sin(\theta_{x,c,p}/2)}\right). \tag{17}$$

Note that for special boundaries ($\theta_{x,c,p} = \theta_x$), the deviation parameter is zero and $\cos(\theta_x/2) = x\sin(\theta_x/2)$, so that the distance between partial secondary dislocations becomes infinite, as expected. Figure 6 shows a plot of δ vs $\theta_{x,c,p}$ as given by Eq. (17) vs misorientation. This exact equation completes, for the whole angular range, the plot of Fig. 6 in Ref. 19, obtained using a small-angle approximation.

The secondary dislocation spacing can also be given in terms of the angular deviation from exact coincidence $\Delta\theta = \theta_x - \theta_{x,c,p}$ as

$$\delta = \frac{\sqrt{2}a}{4}\,\frac{\sin(\theta_x/2)}{\sin(\Delta\theta/2)}. \tag{18}$$

This expression, which has been directly derived from the model, quantitatively reproduces the experimental data of Balluffi *et al.*, summarized in Ref. 19, as is easily verified by comparing its values with the results described therein. Expressing δ in terms of the Burgers vector **b** defined above and $\Delta\theta$, one obtains

$$\delta = \frac{\sqrt{2}}{4}\,\frac{|\mathbf{b}|}{\sin(\Delta\theta/2)}, \quad \delta = \frac{1}{4}\,\frac{|\mathbf{b}|}{\sin(\Delta\theta/2)} \tag{19}$$

for the inclined (x odd) and parallel (x even) states, respectively. If $\Delta\theta \ll 1$, these equations reduce to

$$\delta = \frac{\sqrt{2}}{2}\,\frac{|\mathbf{b}|}{\Delta\theta}, \quad \delta = \frac{1}{2}\,\frac{|\mathbf{b}|}{\Delta\theta} \tag{20}$$

which, replacing $|\mathbf{b}|$ by the more accurate expression $|\mathbf{b}|/2$, coincide for the parallel case with the value for δ given in Eq. (2) of Ref. 19, which disregards the relative orientations of the *O* and CSL lattices.

Knowing that the structure of random twist boundaries is determined by that of its associated singular boundary, it is interesting to enquire as to the angular range over which the structure of singular boundaries extends. Figure 7 shows a semilogarithmic plot of Σ_x vs θ_{arb} illustrating that this range depends monotonically on Σ and that it is larger for smaller Σ.

Note that Eqs. (16)–(20) are independent of the internal variables p and c and contain only observable quantities. Their quantitative agreement with both experimental observations and accepted theory constitutes the strongest piece of evidence in favor of the GCSN model and the hypotheses made therein for the fcc (100) twist case studied here, although the above results are geometrically identical and possibly valid in principle for any cubic system, subject to the constrictions mentioned in previous sections.

As a final word on the structure of random boundaries, we shall mention that their structure is not modified when one crystal is shifted with respect to the other by **b**, the only change being that the two sets of domains interchange positions, the energy of the boundary remaining practically the same after shifting.[11]

In this paper we have chosen the fcc [100] twist case to illustrate the main GCSN model's results and predictions since it is the simplest 2D system that contains all pertinent GB features. However, the model can also be applied as it is to the study of arbitrary crystalline and noncrystalline interfaces, epitaxial systems, and in general, any system for which a 2D boundary can be constructed as prescribed in Sec. II. In particular, the GCSN model can be used to study ionic crystals GB's, where the introduction of vacancies in the boundary has been shown to reduce the interfacial energy[23] to determine the location of such vacancies; when quasicoincident ions have the same charge, they are replaced by an ion of that charge or by a vacancy if the charges are different. These cases shall be the subject of future work.

V. CONCLUSION

In this work the GCSN model has been applied to the study of fcc Twist [100] grain boundaries under the hypothesis that there are at least some real systems whose interatomic potentials minimize interfacial energy as proposed by the model and whose structure is therefore well represented by it. The result has been a set of quantitative expressions obtained directly from the model's hypotheses, concerning primary and secondary dislocation spacings and Burgers vectors that are in complete agreement with both accepted theory and experimental observations. This has provided evidence supporting the above hypothesis, as well as other predictions for which there is no explicit experimental data yet, such as the proposed structure of singular and nonsingular (random) boundaries. Accordingly, singular boundaries, which are defined as those boundaries containing only one primary dislocation per CSL unit cell (or, equivalently, no secondary dislocations), are proposed to be composed of atomic domains with the structure of $\Sigma 1$, separated by an array of perfect primary dislocations. Every random boundary, has an associated singular boundary and its structure consists of a mixture of domains found in the associated boundary in different translational states; these domains are in turn separated by an array of partial secondary dislocations.

In summary, we have in this paper, the following. (a) The detailed atomic structure of GCSN (affine) fcc (100) twist grain boundaries has been obtained in the whole angular range. (b) An unambiguous criterion for singularity, consistent with experimental observations and based entirely on physical (minimum dislocation content) and numerical ($y=1$) grounds, has been proposed. (c) It has been shown that every random GCSN GB has a unique associated singular boundary and a precise association criterion has been given. (d) It has been described how the structure of any random boundary is related to that of its associated singular and the structure of singular (delimiting) GB's consists of atomic domains with 2DSU's of $\Sigma=1$ separated by a network of perfect primary dislocations. (e) It has been shown that the structure of random GCSN GB's consists of mixtures of such domains separated by a network of partial secondary dislocations. (f) The configuration at the atomic level of observed primary and secondary dislocation networks, including dislocation spacings and Burgers vectors, has been obtained and found to be in quantitative agreement with experimental observations.

ACKNOWLEDGMENTS

This work was supported by CONACyT through Grants Nos. 25125-A and 25237-E and by DGAPA (UNAM) through Grants Nos. IN-107296 and IN119698.

[1] A. P. Sutton and R. W. Balluffi, Acta Metall. **35**, 2177 (1987).
[2] D. Wolf and K. L. Merkle, in *Materials Interfaces, Atomic Level Structure and Properties*, edited by D. Wolf and S. Yip (Chapman and Hall, London, 1992).
[3] D. Romeu, L. Beltrán del Rio, J. L. Aragón, and A. Gómez, in *New Horizons in Quasicrystals: Research and Applications*, edited by A. I. Goldman, D. J. Sordelet, P. A. Thiel, and J. M. Dubois (World Scientific, Singapore, 1997), p. 673.
[4] A. Gómez, L. Beltrán del Río, J. L. Aragón, and D. Romeu, Scr. Mater. **38**, 795 (1998).
[5] M. L. Kronberg and F. H. Wilson, Met. Trans. **185**, 501 (1949).
[6] J. L. Aragón, D. Romeu, L. Beltrán del Rio, and A. Gómez, Acta Crystallogr., Sect. A: Found. Crystallogr. **53**, 772 (1997).
[7] For Au and Cu see J. Cai and Y. Y. Ye, Phys. Rev. B **54**, 8398 (1996).
[8] M. Donegan, Ph.D. thesis, University of Surrey, 1976.
[9] K. M. Miller and P. D. Bristowe, Phys. Status Solidi B **86**, 93 (1978).
[10] P. D. Bristowe and S. L. Sass, Acta Metall. **28**, 575 (1980).
[11] D. Romeu and I. Siegal (unpublished).
[12] A. Brokman and R.W. Balluffi, Acta Metall. **29**, 1703 (1981).
[13] W. Bollmann, *Crystal Lattices, Interfaces, Matrices* (Bollmann, Gèneve, 1982).
[14] P. Chaudhari and J. W. Matthews, Appl. Phys. Lett. **17**, 115 (1970).
[15] H. Mykura, P. S. Bansal, and M. H. Lewis, Philos. Mag. A **42**, 225 (1980).
[16] S. Ranganathan, Acta Crystallogr. **21**, 197 (1966).
[17] P. D. Bristowe and A. G. Crocker, Philos. Mag. A **38**, 487 (1978).
[18] W. Bollmann, *Crystal Defects and Crystalline Interfaces* (Springer, Berlin, 1970).
[19] R. W. Balluffi, Y. Komem, and T. Schober, Surf. Sci. **31**, 68 (1972).
[20] V. Vitek and A. P. Sutton, Scr. Metall. **14**, 129 (1980); Philos. Trans. R. Soc. London, Ser. A **309**, 37 (1983).
[21] D. Schwartz, V. Vitek, and A. P. Sutton, Philos. Mag. A **51**, 499 (1985).
[22] P. D. Bristowe and R. W. Balluffi, J. Phys. Colloq. **46**, C4-155 (1985).
[23] P. W. Tasker and D. M. Duffy, Philos. Mag. A **47**, L45 (1983).